

Ingeniería, investigación y tecnología

ISSN: 1405-7743

Universidad Nacional Autónoma de México, Facultad de Ingeniería

Manrique-Negrin, David Azael; Zacarías-Santiago, Alejandro; Guarneros-García, Orlando; Rubio-Ávila, José de Jesús; Pacheco-Martínez, Jaime; Flores-Vasconcelos, Alicia Performance parameters assessment of a pneumatic engine for low capacity commercial vehicles Ingeniería, investigación y tecnología, vol. XXIII, no. 3, e1934, 2022, July-September Universidad Nacional Autónoma de México, Facultad de Ingeniería

DOI: https://doi.org/10.22201/fi.25940732e.2022.23.3.021

Available in: https://www.redalyc.org/articulo.oa?id=40475447005



Complete issue

More information about this article

Journal's webpage in redalyc.org



Scientific Information System Redalyc

Network of Scientific Journals from Latin America and the Caribbean, Spain and Portugal

Project academic non-profit, developed under the open access initiative

Ingeniería Investigación y Tecnología

volumen XXIII (número 3), julio-septiembre 2022 1-13

ISSN 2594-0732 FI-UNAM artículo arbitrado

Información del artículo: Recibido: 15 de octubre de 2021, reevaluado: 24 de enero de 2022,

aceptado: 17 de mayo de 2022

Attribution-NonCommercial-NoDerivatives 4.0 International (CC BY-NC-ND 4.0) license

https://doi.org/10.22201/fi.25940732e.2022.23.3.021



Ingeniería Investigación y Tecnología

Performance parameters assessment of a pneumatic engine for low capacity commercial vehicles

Evaluación de parámetros de rendimiento de un motor neumático para vehículos comerciales de baja capacidad

Manrique-Negrin David Azael

Instituto Politécnico Nacional, ESIME Azcapotzalco, México

E-mail: david.manrique05@gmail.com https://orcid.org/0000-0002-4559-8371

Zacarías-Santiago Alejandro

Instituto Politécnico Nacional, ESIME Azcapotzalco, México

E-mail: azacarias@ipn.mx

https://orcid.org/0000-0002-6427-4911

Guarneros-García Orlando

Universidad Autónoma de San Luis Potosí Departamento de Ingeniería

E-mail: orlando.guarneros@uaslp.mx https://orcid.org/0000-0003-4307-7377 Rubio-Ávila José de Jesús

Instituto Politécnico Nacional, ESIME Azcapotzalco, México

E-mail: rubio.josedejesus@gmail.com https://orcid.org/0000-0002-2005-5979

Pacheco-Martínez Jaime

Instituto Politécnico Nacional, ESIME Azcapotzalco, México

E-mail: jpachecoma@ipn.mx

https://orcid.org/0000-0002-2377-1639

Flores-Vasconcelos Alicia

Instituto Politécnico Nacional, ESCA Santo Tomás, México

E-mail: afloresva@ipn.mx

https://orcid.org/0000-0002-0627-4673

# **Abstract**

In the present work, the performance evaluation of a low capacity pneumatic engine is shown, through modeling and simulation in order to identify the feasibility of its application in commercial vehicles for short distances. For the modeling of the pneumatic engine, the main contribution in this work is that a comprehensive approach has been used including the compressed air supply pipe, the cylinder compression-expansion chamber, and the intake and exhaust valves. The compressed air supply system is modeled using compressible fluid flow models. The fluid flow is considered adiabatic represented by the model known as Fanno flow (or non-isentropic) and it is assumed to be in a steady state. The flow in the opening and exhaust valves are evaluated as adiabatic and isentropic fluid, using a divergent-convergent compressible fluid model. The simulation results show that the feeding pressure and the pipe diameter have a great influence on the motor power. Also, the compression ratio has been found to have strong influence on the overall system efficiency. On the other hand, the simulations show that the initial pressure of the piston does not have a great influence on performance indicators, such as power or efficiency. However, from the results found in this work, it can be seen that the model and all the obtained results can be used to design and generate an optimization model that describes a pneumatic engine proposed for commercial vehicles of low capacity and short distances.

**Keywords:** Pneumatic engine, integral approach, numerical simulation, compressible fluid flow, Fanno flow, commercial vehicles.

### Resumen

En el presente trabajo se muestra la evaluación del desempeño de un motor neumático de baja capacidad, mediante modelado y simulación con el fin de identificar la factibilidad de su aplicación en vehículos comerciales de baja capacidad y distancias cortas. La principal contribución en este trabajo para el modelado del motor neumático, es que se ha utilizado un enfoque integral que incluye la tubería de suministro de aire comprimido, la cámara de expansión y compresión del cilindro, así como las válvulas de admisión y escape. El sistema de suministro de aire comprimido se modela utilizando modelos de flujo de fluido compresible. El flujo de fluido se considera adiabático representado por el modelo conocido como flujo de Fanno (o no isentrópico) y se supone que está en un estado estacionario. El flujo en las válvulas de apertura y escape se evalúa como fluido adiabático e isentrópico, utilizando un modelo de fluido compresible divergente-convergente. Los resultados de la simulación muestran que la presión de alimentación y el diámetro de la tubería tienen una gran influencia en la potencia del motor. Además, se ha descubierto que la relación de compresión tiene una gran influencia en la eficiencia general del sistema. Por otro lado, las simulaciones muestran que la presión inicial del pistón no tiene una gran influencia en los indicadores de rendimiento, como la potencia o la eficiencia. Sin embargo, a partir de los resultados encontrados en este trabajo, se puede apreciar que el modelo y todos los resultados obtenidos se pueden utilizar para diseñar y generar un modelo de optimización que describe un motor neumático propuesto para vehículos comerciales de baja capacidad y distancias cortas.

Descriptores: Motor neumático, enfoque integral, simulación numérica, flujo de fluido compresible, flujo de Fanno, vehículos comerciales.

#### Introduction

Currently, fossil fuels are vital for our global energy needs, accounting for more than 80 % of the world primary energy consumption, IEA (2013). A global fossil fuel study made by Mohr et al. (2015), shows that all the three scenarios analyzed suggest that world coal production may peak before 2025, due to peaking Chinese production, and that only natural gas could have strong growth in the future. The energy consumption and atmospheric emissions of some of the pollutant species reported by Pemex Refinacion under different projections was evaluated by Granados et al. (2021). The authors concluded that is important to develop and apply perspectives than maximize productivity and minimize energy consumption, reducing air emissions. In the last 10 years, the compact and subcompact growth has been higher than most vehicles, close to 100 %. The benefits of the mini-sized electric vehicles were shown by González et al. (2017). The charging of electric vehicles and complementarity of electric vehicles and pumped-hydro as energy storage in small isolated energy systems was investigated by Deflorio et al. (2015), Foley & Gallachoir (2015) and Ramírez et al. (2016), respectively. Can electric vehicles significantly reduce our dependence on non-renewable energy? Scenarios of compact vehicles in the UK are shown by Raugei et al. (2018), Raymand et al. (2021) as a case in point. Studies on alternative fuels using internal combustion engines have been carried out by several authors such as Gugulothu & Reddy (2016) who evaluated In-Cylinder Flow in a diesel engine. Likewise, thermodynamic Analysis of a Turbocharged Diesel Engine Operating under Steady State Condition was carried out by Menacer & Bouchetara (2016). In the same sense, Gómez et al. (2017) and Nguyen & Nguyen (2018) studying the performance of the gasoline-ethanol blend in Otto cycle and motorcycle, respectively.

For the past decade, vehicles using compressed air have been attracting attention. This is due to its low pollution rate and high efficiency, which is comparable to conventional diesel engines. These vehicles could be more efficient if thermodynamic processes are analyzed and modified Zhang *et al.* (2021).

Huang *et al.* (2013) have experimentally studied the performance of a compressed-air driven piston engine. Authors found that the outlet pressure increases at high velocity showing the potential of recycling the compressed air energy by attaching additional cylinders (split-cycle engine). Dimitrova & Maréchal (2015) studied compressed air as an innovative solution for hybridization of small gasoline engine. This powertrain presents the advantage of directly using the shaft of the

engine to transmit the pneumatic torque, generated from the pneumatic energy source - the compressed air tank. A comprehensive review on compressed air powered engine by Marvania & Subudhi (2017) was presented. From the available results, it is evident that with current mechanisms, vehicles powered solely by compressed air cannot be accepted as a practical alternative. Compressed air hybrid propulsion, which combines compressed air propulsion with a conventional internal combustion engine, may be a potential method of avoiding technical failures Fang et al. (2021). Also, Abela et al. (2022) analyzes the pneumatic parameters that compromise a compressed air system in the presence of leaks and mechanical defects, which have a significant impact on its performance. To compensate these limitations, different hybrid pneumatic strategies were evaluated to improve the efficiency. An optimization method for the pneumatic mode of hybrid pneumatic engine by supplying heat during the expansion process of compressed air was carried out by Fang et al. (2018). The results show that the power and torque of the pneumatic prototype engine under the heat source temperature at 90 °C and 1 MPa intake pressure are both increased.

The researchers Huang *et al.* (2009) studied recycling exhaust gas energy of hybrid pneumatic power system with Computational fluids dynamics, CFD. The simulation results show that exhaust gas recycling efficiency and merger flow energy are significantly dependent on the optimum adjustment of the cross-section area, CSA, for changes in air pressure. Under these optimum adjustments, the exhaust gas recycling efficiency can reach about 83 %.

Nowadays, the main objective of pneumatic motor research is to study the design and build viability of pneumatic propulsion for commercial applications, mostly used in motorcycle motors. There are two experimental research studies shown by Wang et al. (2014) and Huang et al. (2013) that investigate the variables that affect the performance of a pneumatic motor. On the other hand, theoretical research studies, refereed in the current paper, aim to simulate a pneumatic system for commercial vehicle application considering only the thermodynamic processes that occur in the piston. The theoretical studies explained in the current paper pursue a numerical simulation of internal piston process and compare them with hybrid pneumatic-combustion systems in the paper of Midhun et al. (2014). Furthermore, Korbut & Szpica (2021) consider that compressed air as a propulsion source, has a disadvantage due to its low air energy density, with very few viable solutions available on the market, which has allowed the development of hybrid systems (combined with other fuels) that can po-

tentially be a good method to avoid technical failures. This agrees with what was stated by Fang et al. (2021), which sees the displacement of a vehicle with a compressed air-only powertrain as difficult, creating the opportunity for the development of work to encourage the search for combined alternative energy sources. Particularly, there is a theoretical study which investigates the performance of a CAV (Compressed Air Vehicle) Papson et al. (2010). It stated the necessity for seeking alternatives to improve CAV performance and for the technology to be competitive among other technologies that are already in the market such as internal combustion, hybrid and electric vehicles. Nabil (2019) transformed a gasoline engine of a motorcycle and incorporated compressed air to drive its different components. Although he warns that the use of low pressure is directly reflected in its driving force, which produces a low performance that hinders its commercialization. Xu et al. (2021) develops a test bench for compressed air vehicles, and analyzes the influence of essential parameters, managing to identify torque and moderate speeds within a competitive economic margin. In conclusion, it has been observed in this study that the CAV has a fuel economy greater than IC cars, but the obtained range is considerably lower than any of the other technologies. The study concludes that the CAV technology has opportunities for improvement in fuel charging and performance; also in order to be competitive it must achieve better efficiency and performance indicators.

This paper aims to assess the performance of a pneumatic engine through modelling and simulation, to identify the viability of its use in commercial vehicles. The main contribution of this work, apart from the cylinder parameters, was to include the feed pipe in the modeling.

#### MODELING

The mathematical modeling is composed of the following 3 main parts: airflow through feeding system, intake valve to the cylinder (opening and closing intake valve, isentropic expansion model), exhaust and remai-

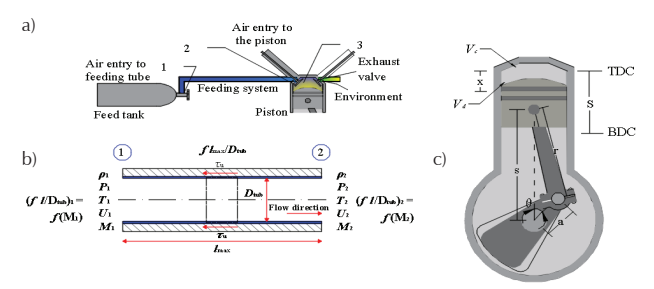


Figure 1. a) Air feeding piping, feeding and exhaust valve, b) Fanno flow in pipe for two points, c) cylinder-piston characteristics

ning (air exhaust, and remaining air compression). Each process is described in this section. The analyzed system we recommend for a compact vehicle.

The main modeling assumptions are:

- · air is modelled as an ideal gas
- adiabatic flow
- steady state flow
- increase in temperature due to friction in the pipeline is not considered

#### AIRFLOW THROUGH FEEDING SYSTEM

The airflow through feeding system process, illustrated in Figure 1a, considers the air entering in the feeding pipe, and in Figure 1b, considers the flow in the pipe, as well as the air compression passing from the cross-sectional area of the intake valve.

This paper models the feeding flow process assuming ideal gas and dividing it into the following subprocesses: feeding Air flow (Fanno Flow; subsonic speeds and adiabatic process) and Convergent flow (isentropic converging-diverging flow; isentropic and adiabatic process). Fanno flow modeling shown by Bar (2018), considers frictional forces interacting inside the pipe as non-isentropic; hence, entropy increases along the pipe. The equation that represents the Fanno flow, uses an average friction factor as follows.

$$\frac{4\bar{f}l_{max}}{D} = \frac{1}{k} \frac{(1-M^2)}{M^2} + \frac{k+1}{2k} \ln\left(\frac{\frac{k+1}{2}M^2}{1+\frac{k-1}{2}M^2}\right)$$
(1)

Where:

 $\overline{f}$  = Fanno friction factor

 $l_{\text{max}}$  = maximum pipe length

D = diameter

 $k = \text{specific heat rate } C_{p}/C_{v}$ 

M = Mach number defined by fluid to sound velocity,<math>M = u/c

For Fanno Flow modeling is convenient to compute the thermodynamic properties in relation to critical properties of the fluid. This is because the friction modifies the stagnation properties at different points of the pipe, whereas the critical properties are those where the speed of the fluid is equal to the speed of sound (M = 1). All the equations will be written as a function of the theoretical stagnation variable.

$$T_0 / T = 1 + (k - 1 / 2) M^2$$
 (2)

here  $T_{\rm o}$  and T are the stagnation and fluid temperature, respectively.

The equations that allow computations of thermodynamic properties along a pipe are Eqs. (3), (4), and (5) for pressure, temperature, and stagnation pressure, respectively:

$$\frac{P}{P^*} = \frac{1}{M} \sqrt{\frac{\frac{k+1}{2}}{1 + \frac{k-1}{2}M^2}} \tag{3}$$

$$\frac{T}{T^*} = \frac{c^2}{c^{*2}} = \frac{\frac{k+1}{2}}{1 + \frac{k-1}{2}M^2} \tag{4}$$

$$\frac{P_0}{P_0^*} = \frac{1}{M} \left( \frac{1 + \frac{k-1}{2} M^2}{\frac{k+1}{2}} \right)^{\frac{k+1}{2(k-1)}}$$
 (5)

where  $P_{o'}$  *P* and c are the stagnation and fluid pressure and sound speed, respectively. The last variable defined by  $c = (kRT)^{1/2}$ . The asterisk \* the critic properties indicate.

Equation (1) is a dimensionless friction factor of Fanno as a function of Mach's number  $4\bar{f} l_{\rm max}/D = f(M)$ . Furthermore, the properties of the pipe must also be known such as pipe diameter,  $D_{\rm tub'}$  pipe length up to point 2, (Figure. 1b),  $l_{\rm max'}$  and friction factor. In order to compute the properties of a second point in the same pipe, we must know the properties of point 1 and the characteristics of the pipe (diameter, length, and friction factor). In this case, it is necessary to compute the properties of point 2, as well as its speed and Mach number. The equation to obtain the calculation of point 2 is the following:

$$\left(\frac{\bar{f}l}{D}\right)_2 = \left(\frac{\bar{f}l}{D}\right)_1 - \frac{4fl_{max}}{D_{tub}} \tag{6}$$

It should not be forgotten that along the pipe, in Fanno model, the mass conservation equation is satisfied. Additionally, pressure drop inside a pipe has a limit, which is known as a critical point,  $P_{\text{limit}}$ ; this is a physical limitation depending on the fluid, and computation of this limit is made with Eq. (7):

$$P_{limit} = P_1 \left(\frac{2}{k+1}\right)^{\frac{k}{k-1}} \tag{7}$$

This physical limit generates a maximum speed that a compressible fluid can achieve due to the differences in pressure inside a pipe line (pressure drop). In the case

that the pressure drop is greater than the critical ratio Eq. (7) Fanno flow model is used to compute fluid speed, meaning speed of sound is not exceeded. In any other condition, moving away from the critical pressure difference condition, the calculation of fluid speed, *U*, at a point in the pipeline was performed using the equation suggested in Mott (2015) and Zacarías *et al.* (2017). The density  $\varrho$  is utilized.

$$U_2 = \sqrt{\frac{2P_1}{\rho_1} \frac{k}{k-1} \left(1 - \frac{P_2}{P_1}\right)^{\frac{k-1}{k}}}$$
 (8)

Intake valve to the cylinder

The expansion model is considered as an adiabatic process. The equation that relates the temperature and the speed of the sound can be written as follows:

$$\frac{T^*}{T_0} = \frac{c^{*2}}{c_h^{*2}} = \frac{2}{k+1} \tag{9}$$

The area that a convergent or convergent-divergent pipe must have to accelerate a fluid at the speed of sound is known as the critical area ( $A^*$ ). The relationship between the cross-sectional area with the critical area and the Mach number is given as:

$$\frac{A}{A^*} = \frac{1}{M} \left( \frac{1 + \frac{k - 1}{2} M^2}{\frac{(k + 1)}{2}} \right)^{\frac{k + 1}{2(k - 1)}} \tag{10}$$

Throughout the convergent or convergent-divergent pipe, the mass conservation is maintained, allowing us to compute through the conservation of matter law the mass flow,  $\dot{m}$ .

$$\frac{\dot{m}}{A} = \frac{kMP_0}{\sqrt{kRT_0}} \left( 1 + \frac{k-1}{2} M^2 \right)^{-\frac{k+1}{2(k-1)}} \tag{11}$$

The average valve opening time allowing air into the piston and the change in mass flow is modelled as a function of the crank angle ( $\theta$ ), variables of piston position (s), and piston instantaneous speed ( $U_p$ ) were used, as shown by Pulkrabek (2014). From Figure 1c, the piston speed is computed as follows:

$$U_p/\overline{U}_p = \frac{\pi}{2} \operatorname{sen} \theta \left[ 1 + \frac{\cos(\theta)}{\sqrt{R^2 - \sin^2 \theta}} \right]$$
 (12)

Where:

$$\overline{U}_p = 2SN \tag{13}$$

$$R = r / a \tag{14}$$

The average velocity is  $\bar{U}_p$ . At 0 crank angle, the piston has an initial mass  $(\dot{m}_o)$ , this mass increases while the intake valve is opened and this was modeled as a function of the mass flow. The initial mass quantity computation is assumed to be ideal gas. The following equation expresses the increase of mass inside the piston as a function of the mass of the piston in the immediate previous degree  $(\theta$ -1).

$$m_{\theta} = m_{\theta-1} + \left(\frac{\dot{m}}{A}\right)_{\theta} A_{\theta} \frac{(s_{\theta} - s_{\theta-1})}{U_p} \tag{15}$$

Where:

$$s_{\theta} = a\cos(\theta) + \sqrt{r^2 - a^2(sen(\theta))^2}$$
 (16)

Particularly, the relative position of the piston is computed with respect to the distance from the centre of the crankshaft to the connection rod of the piston. This is shown in Figure 1 as the variable s.

Once the piston position is known, it is possible to compute the instantaneous piston volume,  $V_d$ , as:

$$V_d = V_c + (\pi B^2/4)(r + a - s)$$
(17)

where  $V_c$  and B are the clearance volume and bore. Thus, it is possible to compute density of the gas, using Eq. (18).

$$\rho_{\theta} = m_{\theta} / V_{\theta} \tag{18}$$

Computing other thermodynamic parameters such as pressure are performed using ideal gas equation.

# ISENTROPIC EXPANSION

The isentropic expansion process begins when the inlet valve is closed. The piston chamber no longer receives more air thus the mass of air inside the piston is constant. Air density is computed considering the density definition.

$$\rho_{\theta} = m_{cte}/V_{\theta} \tag{19}$$

On the other hand, the piston continues to increase its volume, which was computed by Eq. (17). Due to this expansion the density of the air changes in each degree of crank rotation, consequently the pressure and temperature are modified. The process is considered isentropic where the pressure was computed as follows:

$$P_{\theta} = P_{\theta-1} \left( \frac{\rho_{\theta}}{\rho_{\theta-1}} \right)^k \tag{20}$$

PERFORMANCE INDICATORS

Work, w, is the energy that acts in the system at a given distance; it must be computed for a complete cycle, IMEP is defined as the indicated mean effective pressure that is an indication of the operating pressure which the system is working, power is defined as the work done per unit of time,  $\dot{w}$ , torque is an indicator of motor's work of a two strokes IC engine. Equation (21) was used to compute IMEP.

$$IMEP = \dot{W}/V_d \tag{21}$$

This is defined as the force acting on a momentary distance. The torque,  $\tau$ , definition for a one-cycle motor per revolution uses the Eq. (22).

$$\tau = W/2\pi \tag{22}$$

The power, *E*, is computed as Eq. (23).

$$E = W/T (23)$$

Modeling the time this engine, T, takes for one revolution is defined as follows:

$$T = \frac{1}{N(\frac{1min}{60s})} \tag{24}$$

In order to model the efficiency,  $\eta$ , of the engine the definition of (10) is used.

$$\eta = \tau \, \omega / P \, Q \tag{25}$$

Where:

Q = flow rate of compressed air, m<sup>3</sup>/s  $\omega$  = the rotation speed of the engine P = the pressure inlet

#### **EXHAUST AND REMINING**

Air exhaust

Modeling air exhaust is based on considering a small exhaust pipe length, hence pressure at the outlet of the exhaust valve is equal to atmosphere pressure. In the present paper, the throttling occurs due to the exhaust valve pressure and the outlet pressure (atmospheric pressure), this is shown in Figure 1. The difference in pressure between the piston and the atmospheric pres-

sure forces the gas to be throttled in the valve. Before opening the exhaust valve, the conditions of total mass in the piston, pressure, temperature, and density, as well as the atmospheric or outlet pressure of the valve are known. This information is used to compute the output speed with Eq. (9), mass flow, temperature and air outlet density with Eqs. (15), (18), and (2), respectively. Finally, using mass flow it is possible to know mass change inside the piston at any time. As mentioned in case the pressure difference is greater than the critical difference, it must be assumed that the flow is being choked, so that the output speed at the valve will be equal to the speed of the sound (M = 1). Using the equation of the Joule-Thomson Coefficient, the inlet temperature can be computed for the exhaust pipe.

The Joule-Thomson effect,  $\mu_{J}$ , is defined as an isenthalpic process. It is summarized in the following equation according to Vent (2001).

$$\mu_J = \frac{\partial T}{\partial P} = \frac{1}{Cp} \left[ T \left( \frac{\partial V}{\partial T} \right)_P - V \right] \tag{26}$$

Assuming that air behavior follows Van der Waals equation of state, Joule-Thomson coefficient can be written as follows:

$$\mu_J = \frac{\partial T}{\partial P} = \frac{1}{c_P} \left[ \frac{2a}{RT} - b \right] \tag{27}$$

Where a and b are well defined, and they are parameters of the Van der Waals equation for the particular gas.

Once the output speed at the valve and the density of the fluid in the exhaust pipe are known, it is possible to compute the inlet speed in the exhaust pipe through the mass conservation Eq. (15).

# REMAINING COMPRESSION AIR

The process of compressing the remaining air is an isentropic process. This process begins at the moment the exhaust valve is closed, the remaining air is subjected to a compression process in order to reach the nominal working pressure of the piston. The difference between this process and the process of isentropic expansion is that the present process decreases its volume in each movement of the crank, as opposed to the expansion process where it increases.

### RESULTS AND DISCUSSIONS

The model in the programming language Engineering Equation Solver, EES, Klein (2018) was programmed. This software is useful for solving engineering pro-

blems. In order to validate the model proposed in Section 2 for a pneumatic engine, the results were obtained with the engine data shown in Table 1, experimentally obtained by Huang *et al.* (2013) and explained in Manrique (2018). For the simulation, engine parameters shown in Table 2 were utilized. The results for a two-stroke pneumatic motor obtained with the model are shown in this section.

Table 1. Engine characteristics

Parameter	Value
Displacement volume, cm <sup>3</sup> (4-stroke)	101.7
Horsepower, at 7500 rpm, HP	7.5
Torque, at 6000 rpm, N-m	7.44
Bore and stroke, mm	50, 51.8
Compression ratio	10

Table 2. Parameters changed for the simulation

Parameter	Value
Initial pressure, bar	2, 2.5, 3
Compression ratio	5, 10, 20
Intake port, mm	15, 20, 25
Intake pipeline length, cm	20, 30, 50
Feeding valve opening timing. [°]	0 –130, 0 –150, 0 – 170
Exhaust valve opening timing, [°]	150 – 330, 180 – 330, 190 – 330

The results allowed to obtain a graph like the one in Figure 2, where the behavior of the torque, the opening of the intake and exhaust valves, as well as the supply pressure and the pressure inside the cylinder is shown. The Figure shows a behavior very similar to the experimental results published by Huang *et al.* 2013.

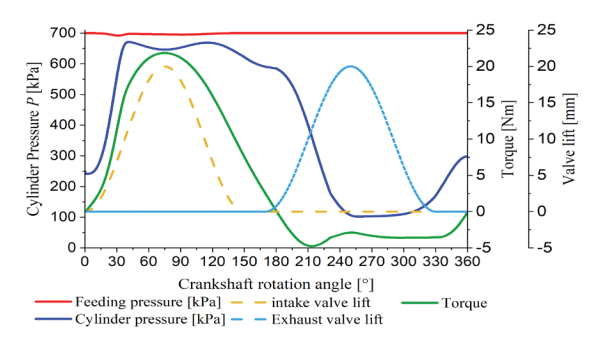


Figure 2. Pressure, admission and exhaust valve and torque *vs* crankshaft rotation angle

The pressure results inside the cylinder published by the author and those found in this work were compared. The error is presented in Figure 3, where it can be seen that the maximum error of the model is 67.2 %, while most of the points have an error of less than 35 %. From this Figure, it can be seen that in thrust, between 0 and 25 degrees of crankshaft rotation, the model has an error of less than 10 %.

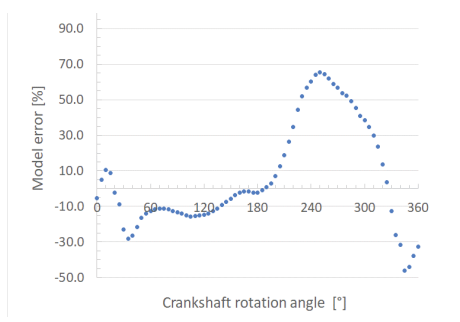


Figure 3. Error in the modeling results, versus experimental results of the literature, from Huang *et al.* (2013)

The comparison of the experimental results from the literature with those obtained in this work, without and with the pipe (improved model), is presented in Figure 4. From this Figure, it can be concluded that, including the supply pipe to the model, the pressure inside the cylinder can increase up to 38.7 % at 25° of crankshaft rotation.

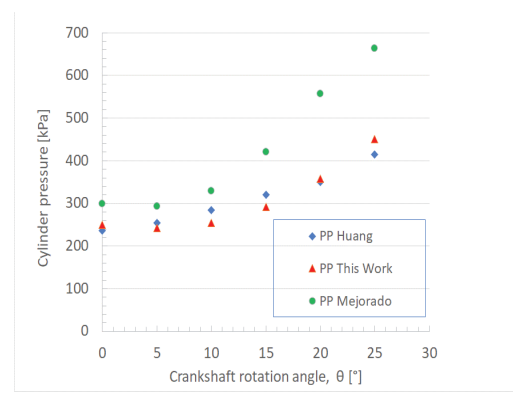


Figure 4. Experimental results from the literature with those obtained in this work, without and with the pipe (improved model)

With these results of the model with an error of less than 10 %, compared to those published in the literature, it was concluded that the model can be used to perform a first assessment of a pneumatic motor operating at different operating conditions, as presented below.

#### AIR FLOW TO FEEDING SYSTEM

The most noteworthy system limitation is fluid speed, which is strongly related by valve opening. Choking

effect is generated during the first 20 crank rotation degrees. This constrains air speed, hence mass entering the piston during the first crank rotation degrees, when pressure difference from piston and feeding pressure is maximum. The choking effect time increases when feeding pressure increases, this is shown in Figure 5. Likewise, it is observed that the speed decreases up to 80 % during the period from 20° to 40° degrees. When speed reaches the point of 40 degrees of rotation, it is observed that the speeds for all cases are equal and this is maintained during the remaining feeding process. An increase in the inlet speed is observed during the remaining degrees of feeding, from 90° onwards, due to the closing of the intake valve.

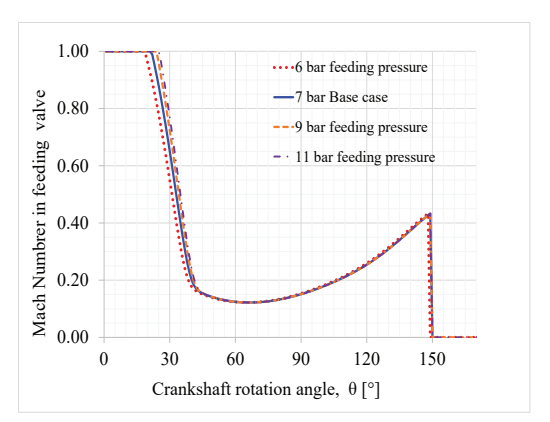


Figure 5. Mach number in feeding valve for each crank rotation angle

It is shown in Figure 6 that torque and power increase considerably when the feeding pressure increases; this is due to the increase in IMEP or average piston pressure. It is observed that the IMEP is below 50 % of feeding pressure. Despite of IMEP increase, system efficiency does not rise significantly. In fact comparing the result of 6 bar feeding pressure of against base case, only an efficiency improvement of 0.35 % is observed. In the case of raising the supply pressure to 9 bar, efficiency increased by 0.42 %. The last case feeding pressure is raised to 11 bar, thus efficiency increases by only 0.25 % compared with 9 bar feeding pressure case.

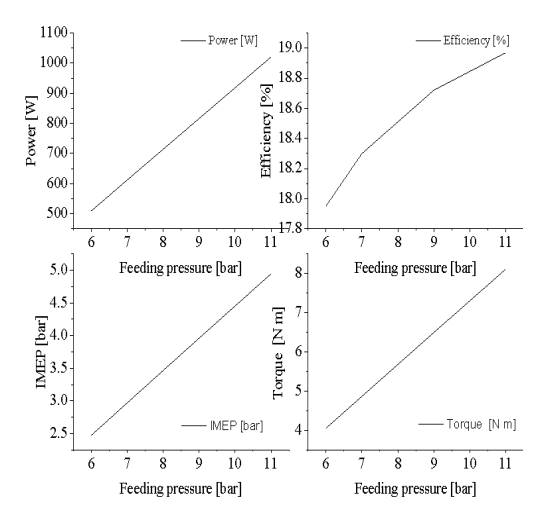


Figure 6. Performance parameters: a) power and efficiency, b) IMEP and torque *vs* feeding pressure

The variables modified and compared with base case scenario were pipe diameter and pipe length. The results are shown in Figure 7. Changes in the feed diameter were simulated by decreasing it by 5mm and later increasing it by 5 millimeters then compared to base case scenario. Modification in feeding pipe length were from base case scenario of 30 cm to 20 cm and then to 50 cm. Simulation results show an improvement in performance indicators and efficiency by increasing the diameter of the pipe by 5 millimeters. The improvement in indicators is 3.2 %, with an increase in efficiency of 0.47 %. As the feed diameter decreased, the results were a decrease in the indicators by 13.5 % and fall in efficiency of 1.93 %.

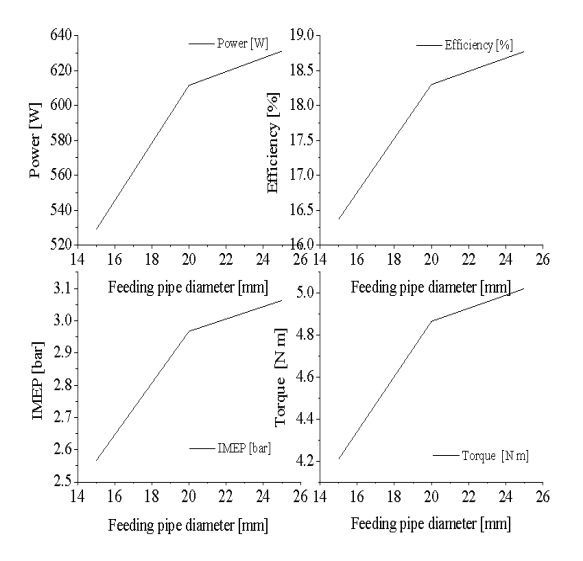


Figure 7. Performance parameters: a) power and efficiency, b) IMEP and torque *vs* feeding pipe diameter

Pipe length changing scenarios in Figure 8 show an improvement on indicators is observed as the length of the pipe is reduced, increasing the indicators such as work, power, torque and IMEP by 2 % and increase efficiency moderately for 0.27 %. The increase in pipe length leads to a drop in the indicators by 1.9 % and a decrease in efficiency of only 0.26 %.

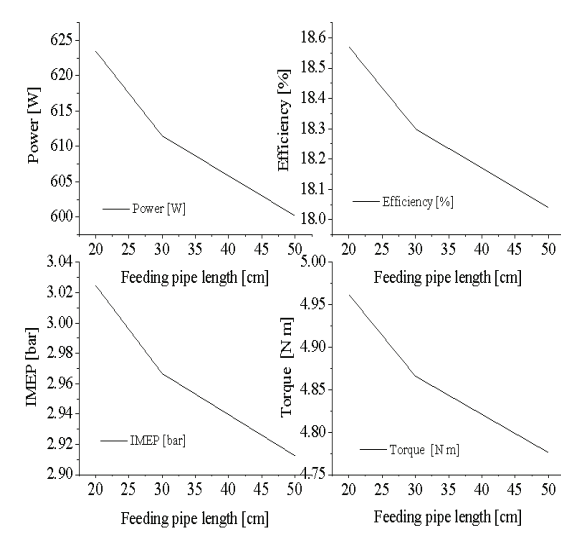


Figure 8. Performance parameters: a) power and efficiency, b) IMEP and torque *vs* feeding pipe length

Decreasing pipe diameter by 5 mm generates a considerable drop in performance indicators; there are two reasons why this effect is so important. First, the indicated mean pressure (IMEP) drops considerably, this effect can be seen in Figure 9 which shows the Pressure-Volume diagram. It is observed that when piston start descending it suffers an important pressure drop, from 640,000 Pa to approximately 520,000 Pa, starting around the 20 cm³ and reaching its minimum in 40 cm³; later, the pressure starts rising. This phenomenon occurs because piston instantaneous speed reaches its maximum value around a crank angle of 70 and 90 degrees, during this interval piston volume is between 20 cm³ and 60 cm³.

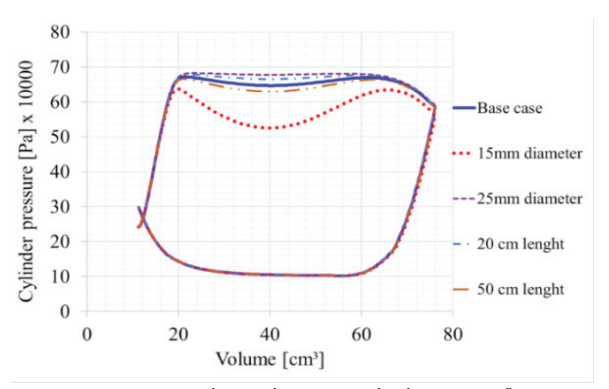


Figure 9. Pressure-volume diagram with changes in flow variables

The pressure drop in the piston is related with system flow restrictions. Hence, in the case when the diameter is the smallest, the volumetric flow is the lowest by about 0.015 kg/s compared to base case. This effect can also be observed in Figure 10. It is clear that the largest mass flow fluctuation occurs during the motor rotation when the system has the lowest tube diameter, from 15 mm. During crank rotation angle interval of 70° to 90° (where the maximum piston speed occurs) the mass flow of the base case with a biggest diameter, 25 mm, is very low compared to the other cases; actually, it can be deduced that the pressure drop is a consequence of the minimum amount of mass entering the system at a rate much lower that the volume increase speed.

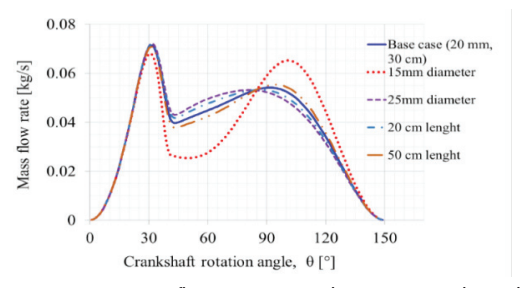


Figure 10. Mass flow rate *vs* crank rotation angle at different flow variables

# INTAKE VALVE TO THE CYLINDER AND COMPRESSION RATIO

Effects on the efficiency results for these cases are due to the flow change. This effect can be seen clearly in Figure 11. This Figure shows that at the beginning of the process between degrees 20 ° and 40 ° the maximum mass flow occurs in each of the shown cases, 0.076 kg/s, 0.0715 kg/s and 0.0662 kg/s for 2 bar, base case and 3 bar respectively. In the same line, for the case of lower initial pressure the maximum mass flow of 0.076 kg/s is the highest, consequently the maximum mass flow for

the upper initial pressure is the lowest, 0.0662 kg/s. This increase in flow is not absorbed by the system in the most efficient way since it is shown before that the flow is not utilized with the highest efficiency, because during this peak on mass flow piston pressure it does not increase significantly. In conclusion, the initial pressure of the piston does not have a significant effect on performance indicators, but it has a positive effect on efficiency. Thus using the highest initial pressure of 3 bar the system can offer the system could operate in a more efficient way.

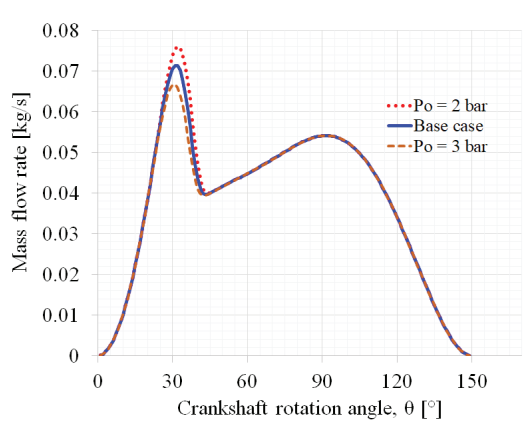


Figure 11. Mass flow rate *vs* crank rotation angle for different initial piston pressure

# Compression ratio influence

The compression ratio has shown to be an important variable for the performance of the motor. The differences in feeding air speed can be seen in Figure 12. This Figure shows that in different rotation degrees there are drastic changes in the feeding speed on the valve. An example of this is to review the results in 30  $^{\circ}$  of rotation where we observe that for a compression ratio of 20 the Mach number is around 0.3, instead for a compression ratio of 10 the Mach number is 0.6, and for the smaller compression ratio (RC 5) the Mach number is 0.9. Having a smaller piston volume, in the case of 20 CR the consequence is that the volume of air entering the piston is up to 66.67 % smaller.

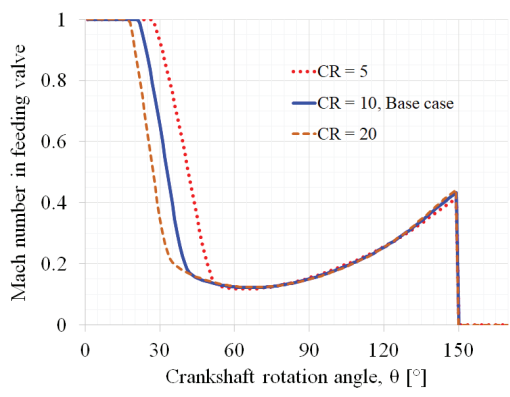


Figure 12. Mach number in intake valve changes with crank rotation angle at different compression ratio

The results of Figure 13 show that the compression ratio has a direct effect on the system efficiency in. However, it does not have significantly affect variables such as Work, Power, or Torque. This indicates that using different CRs to improve variables like work, power or torque would not help. On the other hand, the compression ratio significantly affects the volumetric flow, increasing it in each case, but without obtaining a significance benefit (this is reflected in small IMEP changes).

The positive effect on efficiency due to compression ratio decreases as volume grows. It can be seen that the efficiency increase effect of switching from a CR 5 to a CR 10 (base case) is 2.83 %, while the effect of switching from a CR 10 (base case) to a CR 20 is just 1.19 %. Therefore, the improvement in efficiency is due to the compression ratio having an upper or maximum limit. In conclusion, these results shown that compression ratio has a significant effect on the efficiency of the system. It is advisable to use a smaller volume as the car is driven at higher speeds; this improves the efficiency of the engine, without generating a detrimental effect on the power, work and torque of important consequences.

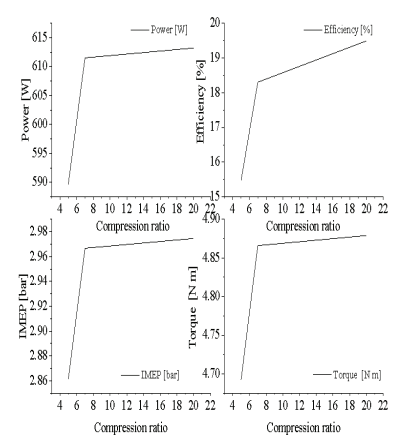


Figure 13. Performance parameters: a) power and efficiency, b) IMEP and torque *vs* compression ratio

#### EXHAUST AND REMAINING

Figure 14 shows the phenomena that rules the mass flow in the different rotation angles. At the beginning of the process the flow rate is governed mainly by the valve opening, since the flow is in a process of convergent flow, so depending on area changes the flow accelerates. This effect shows a mass flow acceleration from 0 kg/s to 0.07 kg/s, between 0° degrees and 30° degrees for the base case. After this process the pressure difference is the phenomenon which governed the fluid speed. This is the reason mass flow is reduced to a minimum, to 0.040 kg/s in 40° degrees. At that minimum point the flow rate continues depending on the pressure difference, but the system undergoes a small pressure drop due to the increased speed of the piston resulting in a greater pressure difference by accelerating the fluid. Finally, a second maximum mass flow of 0.054 kg/s at approximately 90° degrees is observed for the base case; this happens due to a combination of two effects; first, the intake valve decreases its cross-sectional area (it is in the closing stage); secondly, the difference of pressures has decreased considerably generating a rapid drop in fluid speed. This drop in mass flow is maintained until the inlet valve closes completely. Figure 14 shows where highest and lowest mass flow occurs in the case of maintaining the feed valve with 20 ° less.

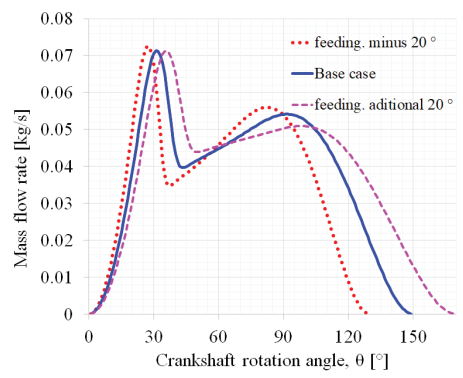


Figure 14. Mass flow rate vs crank rotation angle at different feeding valve opening timing

Comparing the result of base case with the second case, it is observed that the increase in opening time of the exhaust valve adversely affects all the engine performance indicators. The results shown in Figure 15 are compared by the valve opening timing ratio,  $\varphi$ , defined by the exhaust valve opening timing between feeding valve opening timing by the form:

$$\varphi = \frac{\text{exhaust valve opening timing}}{\text{feeding valve opening timing}}$$
(28)

It decreased by 1.4 % the efficiency and affection in about 10 % the performance indicators like work, power, torque and IMEP. On the other hand, when comparing the base case with intake time decrease by 20  $^{\circ}$  an increase of all the performance indicators is observed. These increase by 2.5 %, efficiency increases by 0.35 %.

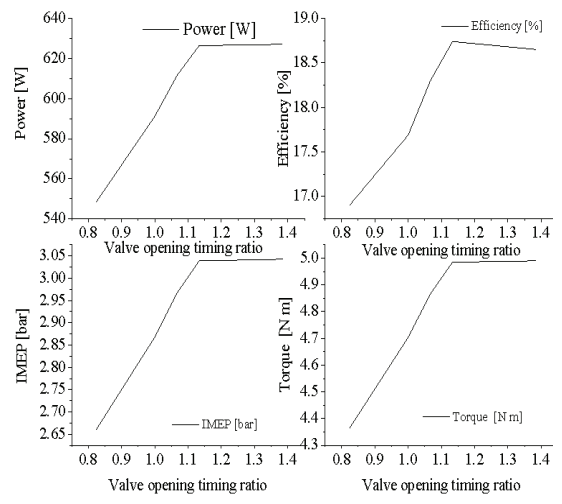


Figure 15. Performance parameters: a) power and efficiency, b) IMEP and torque *vs* exhaust feeding valve opening

# Conclusions

The results of the model and the present study allow the following conclusions:

- The model predicts the power, torque and efficiency results of a pneumatic engine providing the feeding pressure and some flow parameters such as length and diameter of the feeding pipe. This is very useful because the model could be used in the prediction of the performance of pneumatic motors with different operating conditions.
- Influence of feeding pressure on performance variables such as work, power, and torque increase as the piston pressure increases. However, the influence of this on the efficiency of the system is not linear and has an upper limit. Additionally, using a pressure above 9 bars can lead to leakage problems in the system. Hence, this variable has strong limitations in improving system performance. In addition, the energy required to bring a gas to high pressure conditions must be considered.
- The initial pressure of the piston has no significant effect on the performance of the system; thus, designing the highest possible initial pressure value will benefit the system moderately.

- The compression ratio proved to be a key variable to improve the system efficiency. It is demonstrated that this variable can give important benefits to the system in all performance indicators. This paper shows that the greater the compression ratio, the greater the benefit to the efficiency of the system. This variable also has an upper limit to improve efficiency.
- Flow variables such as the diameter and length of the feed pipe proved to have significant effects on the efficiency of the system as well as in the performance indicators. Diameter flow effect proved to have a greater effect on yield than the length of the pipe. It is therefore recommended to use a larger diameter to improve efficiency. Additionally, it is clear that a balance between the speed of the piston and the mass flow must be considered for the design; otherwise, the piston pressure drop will occur causing a significantly decrease of performance.
- Valve opening showed a moderate effect on the system. It is clear that one should look for the shortest admission time as well as the shortest iso-entropic expansion time to improve the system performance. Although it is desirable to allow compressed air to be maintained for the longest time in the system, this effect can be achieved by the choking effect, designing the flow area in the exhaust valve.

It is advisable to make an optimization of the variables above mentioned with a cost benefit study against the efficiency increase of the same system.

#### Nomenclature

position in the system

1, 4	position in the system
а	crank radios (m)
A	Cross-sectional fluid area (m <sup>2</sup> )
В	piston diameter (m)
D	pipe diameter (m)
<u>E</u>	power (W)
f	mean Fanno friction factor
$\overline{f}_L/D$	power (W) mean Fanno friction factor Fanno friction number
ĬMEP	indicative mean effective pressure (Pa)
k	specific heat rate (kJ/kg K)
l	pipe length (m)
m	chamber constant mass (kg)
m	mass flow rate (kg/s)
$(\dot{m}/A)_{\theta}$	mass flow by cross-sectional area in crank an-
	gle $\theta$ (kg/s m <sup>2</sup> )
M	Mach number
N	revolutions per minute (RPM)
P	Fluid pressure (Pa)

connecting rod length (m)

1, 2

R	connecting rod and crank radios rate
S	piston position (m)
3	pistori positiori (iii)
S	career, m
T	Fluid temperature (T)
U	Fluid speed (m/s)
$\overline{Up}$	mean piston speed (m/s)
V	volume (m³)
W	System work (J)
ρ	Fluid density (kg/m³)
τ	torque (Nm)
θ	crank angle (grads)

# **S**UBSCRIPTS

0	stagnation
С	chamber
cte	constant
d	displacement
limit	limit
max	maximum
p	piston
tub	tube
θ	angle
$\theta - 1$	crank angle minus one grad

### SUPERSCRIPTS

\* critical

#### **ACKNOWLEDGEMENTS**

The financial support of this study by the Science research grant 20210293, by the National Polytechnic Institute of Mexico (IPN), is greatly appreciated.

### REFERENCES

- Abela, K., Refalo, P., & Francalanza, E. (2022). Analysis of pneumatic parameters to identify leakages and faults on the demand side of a compressed air system. Cleaner Engineering and Technology, 6, 100355. https://doi.org/10.1016/j.clet.2021.100355
- Bar, G. P. (2013). Fundamentals of compressible fluid mechanics (V. 0.4.9.8). Chicago Illinois.
- Deflorio, F. P., Castello, L., Pinna, I., & Guglielmi, P. (2015). Charge while driving for electric vehicles: road traffic modeling and energy assessment. *Journal of Modern Power Systems and Clean Energy*, 3(2), 277-288.
- Dimitrova, Z., & Maréchal, F. (2015). Gasoline hybrid pneumatic engine for efficient vehicle powertrain hybridization. *Applied Energy*, 151, 168-177. http://10.1016/j.apenergy.2015.03.057
- Fang, Y., Lu, Y., Yu, X., & Roskillyc, A. P. (2018). Experimental study of a pneumatic engine with heat supply to improve the

- overall performance. *Applied Thermal Engineering*, 134, 78-85. https://doi.org/10.1016/j.applthermaleng.2018.01.113
- Fang, Y., Lu, Y., Roskilly, A. P., & Yu, X. (2021). A review of compressed air energy systems in vehicle transport. *Energy Strategy Reviews*, 33, 100583. https://doi.org/10.1016/j.esr.2020.100583
- Foley, A., & Gallachoir, B. O. (2015). Analysis of electric vehicle charging using the traditional generation expansion planning analysis tool WASP-IV. *Journal of Modern Power Systems and Clean Energy*, 3(2), 240-248.
- Gómez, A, Zacarías, A., Venegas, M., Vargas, R. O., Carvajal, I., & Aguilar, J. R. (2017). Modeling and optimization of an otto cycle using the ethanol-gasoline blend. *Revista Mexicana de Inge*niería Química, 16 (3), 1065-1075.
- Granados, E., Alarcón, A. L., López, X., Fuentes, G., Vega, E., Sánchez P., & Sosa, R. (2021). Energy consumption and atmospheric emissions from refined petroleum in Mexico by 2030. *Ingeniería Investigación y Tecnología*, 22 (1), 1-13. https://doi.org/10.22201/fi.25940732e.2021.22.1.002
- Gugulothu, S. K., & Reddy, K. H. C. (2016). CFD Simulation of incylinder flow on different piston bowl geometries in a DI diesel engine. *Journal of Applied Fluid Mechanics*, 9 (3), 1147-1155. https://doi.org/10.18869/acadpub.jafm.68.228.24397
- Huang, C. Y., Hu, C. K., Yu, C. J., & Sung, C. K. (2013). Experimental investigation on the performance of a compressed-air driven piston engine. *Energies*, 6, 1731-1745. https://doi.org/10.3390/en6031731
- Huang, K. D., Quang, K. V., & Tseng, K. T. (2009). Study of recycling exhaust gas energy of hybrid pneumatic power system with CFD. *Energy Conversion and Management*, 50, 1271-1278.
- IEA. World energy outlook; 2013.
- Klein, S. A. (2018) Engineering equation solver. 1992-2018. Academic-professional V10.489 (2018-9-01).
- Manrique, D. A. (2018). Estudio de la mejora en eficiencia de un motor neumático parauso en automóviles comerciales. (MSc Thesis). Instituto Politécnico Nacional, Mexico.
- Korbut, M., & Szpica, D. (2021). A review of compressed air engine in the vehicle propulsion system. *Sciendo*, 5(4). https://doi.org/10.2478/ama-2021-0028
- Marvania, D., & Subudhi, S. (2017). A comprehensive review on compressed air powered engine. *Renewable and Sustainable Energy Reviews*, 70, 1119-1130. https://doi.org/10.1016/j.rser.2016.12.016
- Menacer, B., & Bouchetara, M. (2016). Thermodynamic analysis of a turbocharged diesel engine operating under steady state condition. *Journal of Applied Fluid Mechanics*, 9(2), 573-585. https://doi.org/10.18869/acadpub.jafm.68.225.24661
- Midhun, V. S., Ramesh, A., & Sathyanandan, M. (2014). Comparison of fully pneumatic and pneumatic-electric hybrid configurations for propulsion of a refrigerated vehicle. *Journal of Green Engineering*, 1, 49-70.
- Mott, R. L. (2012). *Applied fluid mechanics*. 4th edition. New Jersey: Pearson
- Nabil, T. (2019). Investigation and implementation of compressed air motorbike engines. Wiley.

- Nguyen-Powered, K., & Nguyen, V. (2018). Study on performance enhancement and emission reduction of used fuel-injected motorcycles using bi-fuel gasoline-LPG. *Energy for Sustainable Development*, 43, 60-67. https://doi.org/10.1016/j.esd.2017. 12.005
- Papson, A., Creutzig, F., & Schipper, L. (2010). Compressed air vehicules. Drive-cycle analysis of vehicules permormance, environmental impact, and economic costs. Transportation Research Record. *Journal of the Transportation Research Board*, 2191, 67-74. https://doi.org/10.3141%2F2191-09
- Pulkrabek, W. W. (2014). Engineering Fundamentals of the Internal Combustion Engine. 2nd Ed. EE UU: Pearson.
- Ramírez, A., Ramos, F. J., & Marrero, G. A. (2016). Complementarity of electric vehicles and pumped-hydro as energy storage in small isolated energy systems: Case of La Palma, Canary Islands. *Journal of Modern Power Systems and Clean Energy*, 4(4), 604-614.
- Raymand, F., Ahmadi, P., & Mashayekhi (2021). Evaluating a light duty vehicle fleet against climate change mitigation targets under different scenarios up to 2050 on a national level. *Ener-gy Policy*, 149, 111942. https://ma.x-mol.com/paperRedirect/1325953997868339200
- Raugei, M., Hutchinson A., & Morrey D. (2018). Can electric vehicles significantly reduce our dependence on non-renewable energy? Scenarios of compact vehicles in the UK as a case in point. *Journal of Cleaner Production*, 201, 1043-1051.
- Vent, S. L. (2001). A summary of properties of van der waals fluids. international. *Journal of Mechanical Engineering Educa*tion, 29 (3), 257-277. https://doi.org/10.7227%2FIJMEE.29.3.8
- Wang, Y. W., You, J. J., Sung, Ch. K., & Huang, Ch. Y. (2014). The applications of piston type compressed air engines on motor vehicles. *Procedia Engineering*, 79, 61-65. https://doi.org/ 10.1016/j.proeng.2014.06.311
- Xu, Y., Zhang, H., Yang, F., Tong, L., Yan, D., Yang, y., Wang, Y., Wu, Y. (2021). Experimental research on universal characteristics and output performance of pneumatic motor for compressed air vehicle. *Journal of Energy Storage*, 41, 102943. http://10.1016/j.renene.2021.07.072
- Zacarías, A., González, J., Granados, A., & Mota, A. (2017). *Mecánica de fluidos: teoría con aplicaciones y modelado*. 1st Ed. Mexico: PATRIA.
- Zhang, X., Wang, X., Li, W., Zhu, Y., Zuo, Z., & Chen, H. (2021). Energy and exergy analysis of compressed air engine systems. *Energy Reports*, 7, 2316-2323. https://doi.org/10.1016/j.egyr.2021.04.025

### Cómo citar:

Manrique-Negrin D. A., Zacarías-Santiago A., Guarneros-García O., Rubio-Ávila J. de J., Pacheco-Martínez J., & Flores-Vasconcelos A. (2022). Performance parameters assessment of a pneumatic engine for low capacity commercial vehicles. *Ingeniería Investigación y Tecnología*, 23 (03), 1-13. https://doi.org/10.22201/fi.25940732e.2022.23.3.021